# Late-Time Potential Shallowing and Low-Acceleration Hints: A Minimal Scalar-Refractive Interpretation with Laboratory Falsifiability

Gary Alcock

October 1, 2025

**Abstract**

Several recent measurements continue to stress General Relativity (GR) in the late-time universe. First, a model-independent, direct measurement of the Weyl gravitational potential from DES Year 3 weak-lensing $\times$ clustering finds the lowest-redshift bins are *2–3$\sigma$ shallower* than $\Lambda$CDM+GR expectations. Second, DESI DR2 BAO—in combination with supernovae and a CMB distance prior—exhibit *dataset-dependent* preference for dynamical dark energy over a pure cosmological constant. Third, independent, late-time determinations of $H_0$ (time-delay cosmography; JWST-Cepheid cross-checks of the local distance ladder) keep the Hubble tension alive as a robust cross-method discrepancy. In parallel, *Gaia* wide-binary tests at accelerations $\lesssim 10^{-10}\,\mathrm{m\,s^{-2}}$ remain active and contested. We show that a minimal scalar refractive framework—in which photons see an optical index $n = e^{\psi}$, matter accelerates as $\mathbf{a} = (c^2/2)\nabla\psi$, and $\psi$ obeys a quasilinear Poisson equation with a low-acceleration crossover—naturally yields (i) time-weakening lensing potentials as the mean density dilutes and (ii) MOND-like phenomenology in the deep-field regime, while (iii) remaining indistinguishable from GR in Solar-System PPN tests and (iv) offering a decisive, laboratory falsifier via clock redshift comparisons between *solid-state cavities* and *atomic transitions*. We emphasise these observations as *motivations*, not proofs; the laboratory discriminator carries the ultimate burden of evidence.

## 1 Introduction

GR remains extraordinarily successful in high-gradient and Solar-System regimes. At late times and low accelerations, however, several independent datasets continue to show mild but persistent tensions with $\Lambda$CDM+GR. Most notable are: (i) the DES Y3 *direct* Weyl-potential measurement showing shallower low-$z$ wells; (ii) DESI DR2 BAO combinations indicating a dataset-dependent preference for $w(z) \neq -1$; (iii) the durability of the $H_0$ split across methods (distance ladder with JWST cross-checks, time-delay cosmography). At the same time, wide-binary tests of gravity at $a \sim 10^{-10}\,\mathrm{m\,s^{-2}}$ remain contested and under active refinement. We ask a restricted, operational question: can a *minimal* scalar refractive picture capture the *qualitative* directions of these anomalies while staying fully compliant with PPN constraints and yielding an unambiguous, lab-grade falsifier?

## 2 Minimal scalar-refractive framework

We consider a single scalar field $\psi(\mathbf{x})$ defining an optical medium

$$n(\mathbf{x}) = e^{\psi(\mathbf{x})}, \qquad c_1(\mathbf{x}) = \frac{c}{n} = c\,e^{-\psi}, \tag{1}$$

with the weak-field matter response

$$\mathbf{a} = \frac{c^2}{2}\nabla\psi \equiv -\nabla\Phi, \qquad \Phi \equiv -\frac{c^2}{2}\psi, \tag{2}$$

and a quasilinear field equation with a single crossover function $\mu$:

$$\nabla\cdot\big[\mu(|\nabla\psi|/a_\star)\,\nabla\psi\big] = -\frac{8\pi G}{c^2}\,\big(\rho-\bar{\rho}\big). \tag{3}$$

Here $a_\star$ sets the low-acceleration crossover. The normalisation is chosen so that in high-gradient regimes ($\mu \to 1$) one recovers the Newtonian potential and all 1PN optical tests of GR (light deflection, Shapiro delay) exactly. In the deep-field regime, $\mu(x) \sim x$ yields $|\nabla\psi| \propto 1/r$ and asymptotically flat rotation curves, i.e. MOND-like phenomenology, without adding dark matter explicitly. This construction is *minimal*: a single scalar with a single interpolation $\mu$.

### Action principle, coupling, and PPN limit

To address physical mechanism and avoid ad hoc postulation, consider the action

$$S = \int d^4x\,\sqrt{-g}\left[\frac{c^4}{16\pi G}\,a_\star^2\,\mathcal{H}\!\left(\frac{|\nabla\psi|}{a_\star}\right) - \psi\,(\rho-\bar{\rho})\right] + S_{\rm SM}\big[e^{-\psi}A_\mu,\ \Psi_{\rm matter}\big]\,. \tag{4}$$

Here $\mathcal{H}$ is a dimensionless function and $S_{\rm SM}$ denotes the Standard-Model sector with photons coupled through the optical metric (phase velocity $v_{\rm phase} = c\,e^{-\psi}$) while massive fields follow the weak-field acceleration law above. Varying (4) with respect to $\psi$ yields

$$\nabla\cdot\left[\mu\!\left(\frac{|\nabla\psi|}{a_\star}\right)\nabla\psi\right] = -\frac{8\pi G}{c^2}\,(\rho-\bar{\rho}), \qquad \mu(y) \equiv \frac{1}{y}\,\frac{d\mathcal{H}}{dy}. \tag{5}$$

Thus the interpolation $\mu$ is generated by a single scalar functional $\mathcal{H}$; the limits $\mu\to 1$ (high gradient) and $\mu \sim y$ (deep field) follow from $\mathcal{H}$ being quadratic for $y \gg 1$ and $\propto y^2/2$ for $y \ll 1$, respectively. *PPN sketch.* Expanding (4) around a static, weak-field source with $g_{\mu\nu} = \eta_{\mu\nu} + \delta g_{\mu\nu}$ and $\psi \ll 1$, one finds to $\mathcal{O}(v^2/c^2)$ that $g_{00} = -1 + 2\Phi/c^2 + \mathcal{O}(c^{-4})$ and $g_{ij} = \delta_{ij}\,(1 + 2\Phi/c^2) + \mathcal{O}(c^{-4})$ with $\Phi = -\frac{c^2}{2}\psi$ sourced by (3). Hence light deflection and Shapiro delay correspond to $\gamma = 1$, and the quadratic response of $\mathcal{H}$ in the high-gradient limit yields $\beta = 1$ at 1PN order; preferred-frame/non-conservative PPN parameters vanish at leading order.

### Units and normalization of $\mu$

Because $\psi$ is dimensionless, $|\nabla\psi|$ has units of inverse length. It is convenient to write the argument of $\mu$ in terms of the *acceleration* $a \equiv (c^2/2)\,|\nabla\psi|$:

$$x \;\equiv\; \frac{|\nabla\psi|}{(2a_\star/c^2)} \;=\; \frac{a}{a_\star}.$$

With this choice, the interpolation $\mu(x)$ is a function of $a/a_\star$ as in standard MOND-like notation, while Eq. (3) retains the form given.

### Interpolation $\mu(x)$ and the scale $a_\star$

Representative choices that capture both regimes are

$$\mu_{\rm simple}(x) = \frac{x}{1+x}, \qquad \mu_{\rm standard}(x) = \frac{x}{\sqrt{1+x^2}}. \tag{6}$$

Both satisfy $\mu \to 1$ for $x \gg 1$ and $\mu \sim x$ for $x \ll 1$. The scale $a_\star$ is not a fine-tuned constant but encodes the transition from linear (Newton/GR) response to the deep-field regime; phenomenologically, $a_\star \sim 10^{-10}\,\mathrm{m\,s^{-2}}$ brackets the galactic crossover and is precisely where wide-binary tests are probing.

## 3 Late-time potential shallowing (DES)

GR+$\Lambda$ anticipates nearly constant late-time gravitational potentials on large scales; departures are typically ascribed to evolving dark energy or modified growth functions. DES Y3 report a *direct*, model-independent estimate of the Weyl potential in four redshift bins using combined galaxy-galaxy lensing and clustering; the two lowest-$z$ bins are measured $\sim 2\sigma$ and $\sim 2.8\sigma$ below $\Lambda$CDM expectations. In Eq. (3), the source of $\psi$ tracks $(\rho - \bar\rho)$. As the universe dilutes, the line-of-sight mean approaches $\bar\rho(t)$ and the typical $\psi$-gradient weakens, leading generically to shallower lensing potentials at late times:

$$\frac{\Delta\Phi}{\Phi} \sim \frac{\Delta\rho}{\rho} \quad \Rightarrow \quad \text{late-time shallowing as } \rho\downarrow. \tag{7}$$

*Quantitatively*, the DES low-$z$ deficit corresponds to a fractional reduction at the $\mathcal{O}(10\%)$ level (consistent with a 2–3$\sigma$ deviation when mapped to the fiducial covariance), which is the expected order from modest dilution of the large-scale $\psi$-gradient without invoking exotic microphysics. This qualitative trend matches the DES finding and requires no exotic dark-energy microphysics beyond the effective refractive response of the cosmic medium.

### FRW implementation

Write $\psi(\mathbf{x},a) = \bar\psi(a) + \delta\psi(\mathbf{x},a)$ and $\rho = \bar\rho(a)\,[1+\delta(\mathbf{x},a)]$ in a spatially flat FRW background with scale factor $a$. In comoving coordinates, $\nabla^2_{\rm phys} = a^{-2}\nabla^2$. Assuming $\mu$ is slowly varying

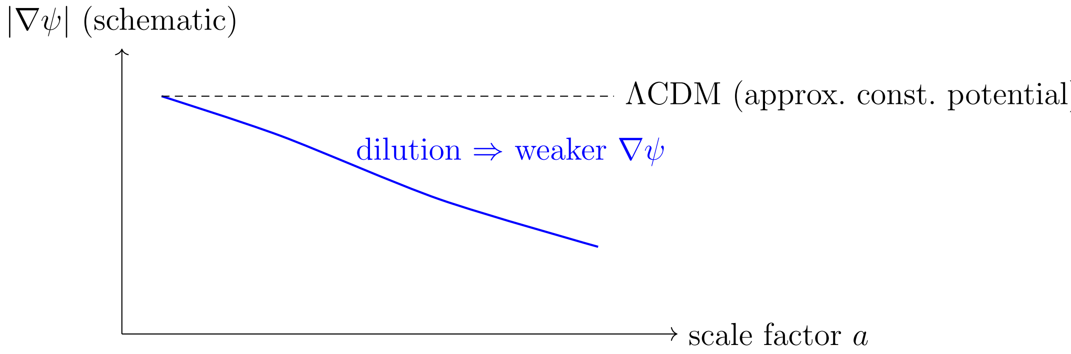


Figure 1: Schematic comparison: the scalar-refractive picture generically weakens the line-of-sight $\psi$-gradient with cosmic dilution, producing shallower late-time lensing potentials than a strictly constant-potential baseline.

on the large scales of interest, one obtains at linear order and in the quasistatic regime ($k \gg aH$):

$$\mu(\bar{x})\,\nabla^2\delta\psi \;\simeq\; -\frac{8\pi G}{c^2}\,a^2\,\bar{\rho}(a)\,\delta(\mathbf{x},a), \qquad \delta\Phi \equiv -\tfrac{c^2}{2}\delta\psi. \tag{8}$$

Hence

$$\delta\Phi_k(a) \;\propto\; \frac{a^2\,\bar{\rho}(a)\,D(a)}{\mu(\bar{x}(a))\,k^2}, \tag{9}$$

with $D(a)$ the linear growth factor. In GR ($\mu = 1$) this reduces to the familiar result: $\delta\Phi$ roughly constant in matter domination and decaying once dark energy dominates. In the scalar-refractive picture, any *secular drift* of $\mu(\bar{x}(a))$ due to the slow evolution of the background $|\nabla\psi|$ produces an additional, controlled decay factor. **Toy parametrization.** Taking $\mu^{-1}(\bar{x}(a)) = 1 + \epsilon_0\,[a/a_t]^p$ with $(\epsilon_0, p) \sim (0.1, 1)$ and $a_t \sim 0.7$ yields a $\sim$10% reduction in $\delta\Phi$ between $z \approx 0.6$ and $z \approx 0.2$, consistent in order-of-magnitude with DES. We present this as a toy *$\mu$–evolution* model; a full Boltzmann treatment is left for future work.

# 4 Dynamical late-time background (DESI DR2, cautiously)

DESI DR2 BAO, when combined with SNe and a CMB distance prior, shows a *dataset-dependent* preference for dynamical dark energy $w(z)$ over $\Lambda$. We treat this not as proof of new physics but as convergent motivation: late-time geometry appears flexible enough that a refractive description—in which optical path-lengths are effectively $D_{\rm opt} = \frac{1}{c}\int e^{\psi} ds$—can account for mild departures from a rigid-$\Lambda$ background without compromising early-time CMB fits. *Toy model.* For small $\psi$, $D_{\rm opt} \approx \frac{1}{c}\int(1+\psi)\,ds$ so the inferred distance-redshift relation acquires a fractional bias $\Delta D/D \simeq \langle\psi\rangle_{\rm LOS}$. Parametrising $\langle\psi\rangle_{\rm LOS}(z)$ by a smooth function (e.g. a cubic spline anchored at the DESI effective redshifts) induces an *effective* $w(z)$ in standard fits without invoking a fluid; small, percent-level $\psi$ biases can mimic mild dynamical-$w$ preferences in the same redshift range, consistent with the cautious language used here.

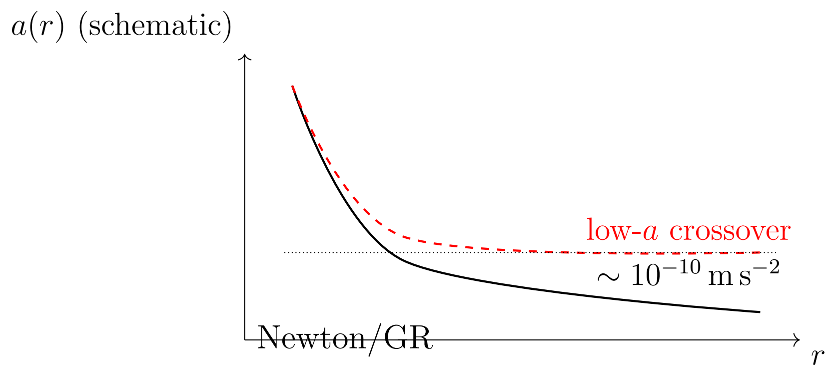


Figure 2: Illustrative acceleration profiles: a low-$a$ crossover (dashed) flattens relative to Newton/GR (solid) near $a \sim 10^{-10}\,\mathrm{m\,s^{-2}}$. Wide-binary studies currently disagree over the presence of such a deviation.

# 5 Low-acceleration regime (wide binaries; active and contested)

*Gaia* wide binaries probe internal accelerations down to $a \sim 10^{-10}\,\mathrm{m\,s^{-2}}$. Some analyses report a ∼20% velocity excess beyond ∼3000 au consistent with MOND-like expectations; others demonstrate that realistic triple-population modelling and stricter data cuts drive the signal back toward Newtonian dynamics. Given current disagreement, wide binaries are best viewed as an *active, near-term battleground* precisely at the scale where Eq. (3) transitions ($\mu \sim x$). For orientation, the $\mu$-**crossover radius** follows from $x = a/a_\star \simeq 1$. Using $a = (c^2/2)|\nabla\psi|$ and the point-mass high-gradient solution $|\nabla\psi| = 2GM/(c^2 r^2)$, one has $a = GM/r^2$ and $x = GM/(a_\star r^2)$. Thus the crossover radius is

$$r_\times = \sqrt{\frac{GM}{a_\star}} \approx 7.1 \times 10^3\,\mathrm{au} \left(\frac{M}{M_\odot}\right)^{1/2} \left(\frac{1.2 \times 10^{-10}\,\mathrm{m\,s^{-2}}}{a_\star}\right)^{1/2}, \tag{10}$$

i.e. $(3\text{–}7) \times 10^3$ **au** for $M \sim (0.2\text{–}1)M_\odot$, matching the observational dispute range now under scrutiny. Our point is limited: the *direction* of the disputed anomaly aligns with the minimal scalar-refractive crossover.

# 6 Consistency and counter-evidence

Any alternative must squarely face null tests. A key geometry vs. dynamics test, $E_G$, has recently been measured with ACT DR6 CMB-lensing × BOSS galaxies and found *consistent* with ΛCDM/GR and largely scale-independent within current precision. Weak-lensing $S_8$ results have also evolved: the KiDS-Legacy cosmic-shear analysis is *consistent* with Planck ΛCDM. These findings do not contradict the qualitative late-time trends above, but they emphasise caution: late-time tensions are uneven across probes and evolving with improved analyses.

## Quantitative benchmarks and laboratory error budget

**Cavity–atom slope (decisive prediction).** For two stationary platforms separated by $\Delta h$, the gravitational potential difference is $\Delta\Phi \simeq g\,\Delta h$. The scalar-refractive picture yields a *ratio* redshift between an evacuated optical cavity (tracking $v_{\text{phase}} = c\,e^{-\psi}$) and a co-located atomic transition:

$$\left.\frac{\Delta f}{f}\right|_{\text{cav/atom}} = \boldsymbol{\kappa}\,\frac{\Delta\Phi}{c^2}, \qquad \boxed{\kappa = 1 \text{ (scalar refractive)}}, \quad \kappa = 0 \text{ (GR)}. \tag{11}$$

*Derivation of* $\kappa = 1$. Locally, $f_{\text{cav}} \propto v_{\text{phase}}/(2L) \propto e^{-\psi}$ (with $L$ a proper length stabilized against elastic sag). Thus $\Delta f_{\text{cav}}/f_{\text{cav}} = -\Delta\psi$. Using $\Phi = -\frac{c^2}{2}\psi$, one has $\Delta\psi = -2\,\Delta\Phi/c^2$ so $\Delta f_{\text{cav}}/f_{\text{cav}} = +2\,\Delta\Phi/c^2$. Atomic transitions redshift with proper time, $\Delta f_{\text{at}}/f_{\text{at}} = +\Delta\Phi/c^2$ to leading order. Therefore for the *ratio* $R = f_{\text{cav}}/f_{\text{at}}$ across two heights:

$$\frac{\Delta R}{R} = \left(\frac{\Delta f}{f}\right)_{\text{cav}} - \left(\frac{\Delta f}{f}\right)_{\text{at}} = (2 - \ 1)\,\frac{\Delta\Phi}{c^2} = \frac{\Delta\Phi}{c^2},$$

i.e. $\kappa = 1$. With $\Delta h = 100$ m and $g \simeq 9.81\,\mathrm{m\,s^{-2}}$,

$$\frac{\Delta f}{f} \approx \frac{g\,\Delta h}{c^2} \approx 1.1\times 10^{-14} \ \text{ per 100 m}, \tag{12}$$

providing a clear target for present-day optical metrology. A cross-material (e.g. ULE vs. Si) and cross-species (e.g. Sr vs. Yb) ratio design isolates the universal geometry-locked slope from material dispersion or atomic structure.

**DES shallowing (order-of-magnitude).** Mapping the reported 2–3$\sigma$ low-$z$ deficit to fractional amplitude implies $\mathcal{O}(10\%)$ weaker Weyl potential than the Planck-$\Lambda$CDM expectation in those bins, consistent with dilution of $\nabla\psi$ along typical lines of sight.

**Wide-binary crossover (orientation).** For a solar-mass system, $a = GM/r^2$ crosses $\sim 10^{-10}\,\mathrm{m\,s^{-2}}$ for separations of order $(3\text{–}7)\times 10^3$ **au**, overlapping the regime where Gaia analyses disagree.

| **Scale / Probe** | **Prediction (scalar refractive)** | **Status** |
|---|---|---|
| Solar System (PPN) | $\gamma = \beta = 1$; preferred-frame $\approx 0$ | GR-consistent |
| DES (low-$z$ Weyl) | $\Delta\Phi/\Phi = \mathcal{O}(10\%)$ shallower | 2–3$\sigma$ low at low $z$ |
| Galactic rotation | $\lvert\nabla\psi\rvert \propto 1/r$; flat $v$; TF scaling | Empirical trend |
| Wide binaries | Crossover near $a_\star \sim 10^{-10}\,\mathrm{m\,s^{-2}}$ | Active, contested |
| Lab (100 m) | $(\Delta f/f)_{\text{cav/atom}} \approx 1.1\times 10^{-14}$ | Near-term falsifier |

Table 1: Representative quantitative benchmarks across regimes.

# 7 Laboratory falsifiability (decisive path)

The decisive test is local and composition-resolved. In a verified nondispersive band, a vacuum optical cavity's resonance frequency scales with the phase velocity $v_{\mathrm{phase}} = c/n = c\,e^{-\psi}$, while co-located atomic transition frequencies track internal energy intervals. Comparing a cavity to an atomic clock at two different gravitational potentials isolates a *ratio* redshift: GR predicts a strict null (both redshift equally), whereas the scalar-refractive picture allows a small, geometry-locked slope $\propto \Delta\Phi/c^2$. A cross-material, cross-species ratio protocol cleanly separates material/atomic systematics; the observable is route- and potential-dependent, not device-dependent. This experiment carries the model's risk: a strict null at laboratory sensitivity falsifies the framework.

# Embedding and symmetry remark

While the present work stays agnostic about a full high-energy completion, Eq. (4) sketches a minimal embedding: a single scalar controlling the optical metric seen by photons and sourcing an effective potential for matter. Deep-field universality arises from the single interpolation function $\mu(x)$; no multiple free functions are introduced. The $\mu \sim x$ behaviour reflects an emergent scale-free response in the $|\nabla\psi| \ll a_\star$ sector rather than fine-tuning a specific exponent.

# 8 Conclusions

We have outlined a minimal scalar-refractive model that: (i) matches Solar-System PPN constraints; (ii) *qualitatively* reproduces late-time potential shallowing as the universe dilutes and a low-$a$ crossover phenomenology at $a \sim 10^{-10}\,\mathrm{m\,s^{-2}}$; (iii) remains decisively falsifiable via laboratory cavity–atom redshift ratios. We regard current cosmological anomalies as *motivations*, not conclusions. If future DESI/LSST-era analyses strengthen dynamical late-time signals while $E_G$ and shear constraints continue to tighten, the scalar-refractive picture will face sharper quantitative tests. Regardless, the laboratory ratio test provides a clean decision procedure independent of cosmological systematics.

# References

**DES Weyl potential (model-independent)**: I. Tutusaus *et al.*, "Measurement of the Weyl potential evolution from the first three years of Dark Energy Survey data," *Nature Communications* **15**, 9295 (2024).

**DESI DR2 dynamical $w$ (dataset-dependent)**: S. Adil *et al.*, "Dynamical dark energy in light of the DESI DR2 BAO," *Nature Astronomy* (2025); see also arXiv:2504.06118 (updated 2025) for a data-combination analysis consistent with the journal version.

$H_0$ **status (independent late-time anchors)**: S. Birrer *et al.* (TDCOSMO), "Cosmological constraints from strong lensing time delays," arXiv:2506.03023 (2025) and references therein; L. Breuval *et al.*, "Latest updates on the Hubble tension from JWST by the SH0ES team," AAS 246 (2025), abstract; see also contemporaneous JWST-based coverage confirming HST Cepheid

calibrations.
$E_G$ **gravity test (GR-consistent)**: L. Wenzl *et al.*, “The Atacama Cosmology Telescope DR6: gravitational lensing × BOSS $E_G$ test,” *Phys. Rev. D* **111**, 043535 (2025).
**KiDS-Legacy shear (Planck-consistent)**: B. Stölzner *et al.*, “KiDS-Legacy: Consistency of cosmic shear measurements with Planck,” arXiv:2503.19442 (2025).
**Wide binaries (active & contested)**: C. Pittordis & W. Sutherland, “Wide binaries from Gaia DR3: testing GR vs. MOND with realistic triple modelling,” *Open Journal of Astrophysics* (2025); X. Hernandez, “A recent confirmation of the wide binary gravitational anomaly,” *MNRAS* **537**, 2925 (2025).